ONLINE SUPPLEMENT

Supplementary to Lauri et al: *Future changes in Mekong River hydrology: impact of climate change and reservoir operation on discharge*.

S1 Reservoir optimisation method

To define reservoir operation, a linear programming (LP) optimisation was used to define monthly outflows for each reservoir separately. The target of the objective function is to maximise annual outflow from a reservoir through hydropower turbines, using the reservoir active storage, estimated monthly inflows, minimum outflow, and optimal outflow from the reservoir as parameters. The problem was defined as follows:

Variables:

q_i	monthly outflow from reservoir
o_i	monthly overflow from reservoir
qin_i	estimated monthly inflow, i=1..12
s_i	reservoir active storage, i=1..12
$qmin_i$	minimum value for outflow, i=1..12
qopt	maximum flow through turbines
smax	reservoir active storage
k	parameter for storage water level
sign(x)	function, returns -1 if x<0, else +1
nd_i	days in month i, i=1..12

Objective (i=1..12):

$$\text{Max } \Sigma \ (q_i \ + k \ \text{sign}(qopt - qin_i))$$

Constraints (i=1..12):

1) $s_i + s_{i+1} + nd_i \ (qin_i - q_i - o_i) = 0$;
2) $q_i > qmin_i$
3) $q_i < qopt$
4) $s_i < smax$
5) $q_m = q_n$; m,n = 1,2; 2,3; 3,4; 4,5.

The above optimisation problem can be solved using standard linear programming methods. As results, optimised monthly outflows q_i and reservoir storage values s_i are obtained for each month. The term starting with coefficient *k* in the objective function aims to maximise reservoir storage when the inflow is larger than optimal flow (wet season), and minimise storage when the inflow is lower than optimal flow (dry season). This forces the filling of the reservoir during the wet season, end the emptying of the reservoir during the dry season. Additional equality constraints (5) were added to keep the reservoir outflow constant during the dry season. Coefficient k can be adjusted, but here k was set to average inflow to reservoir times 10^{-6}.

To regulate the daily outflow of a dam, the computed data were used as follows:

Variables:

- c current active storage
- q_{out} current outflow
- q_{id} interpolated outflow
- s_{id} interpolated storage

Algorithm:

if $c > s_{id}$ then $q_{out} = q_{id}$

if $c < s_{id}$ then $q_{out} = q_{id} (c/s_i)^2$

The monthly inflows to each reservoir were estimated from computed 24-year time series (1981-2005) for each reservoir. These monthly inflows were then reduced by multiplying the data with coefficient **r**, in order to reduce the amount of years when the reservoir would not completely fill up due to lack of water. Coefficient **r** was computed as **(a-0.75 s)/a**, where **a** is the average annual inflow, and **s** the standard deviation of average annual flows. The minimum flow for each month was set to be 0.25 times the average annual flow, but no larger than 0.25 times the average monthly inflow.

Using the above defined operation rules the reservoir storages typically fill up about every second year. Normal reservoir operation rules are more careful and aim to make certain that the reservoir is filled up to full capacity each year. Here, however, the aim was to find an upper limit of the possible impacts of reservoirs on Mekong discharge.

The optimisation of all reservoirs was performed so that before optimising a given reservoir, all of the other reservoirs upstream from it were the upstream reservoirs were optimised. The inflows to the reservoir to be optimised were then computed with the upstream reservoirs active. An example of a reservoir regulation result is shown in Fig. S1, which displays the water level of the Chinese Xiaowan reservoir. The reservoir reaches full capacity on 17 of the 24 simulated years, and reaches the minimum operating level three times.

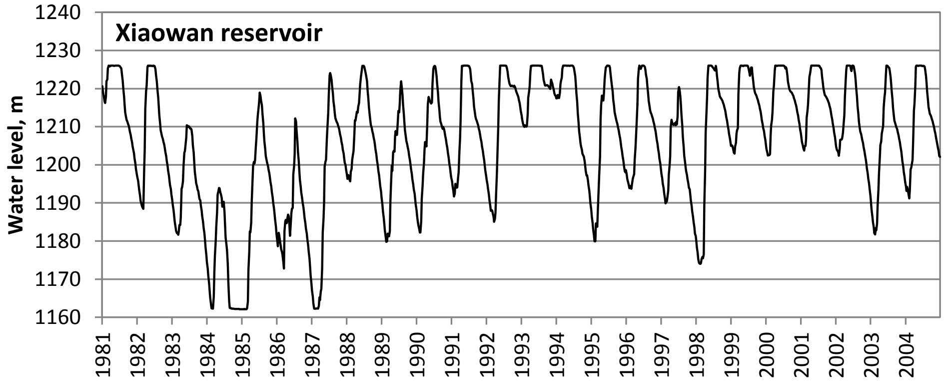

Figure S1: An example of a reservoir operation rule result: computed Xiaowan reservoir water level for years 1981-2005.

S2 Evapotranspiration computation

Potential evaporation is computed using the Hargreaves-Samani evaporation formulation (Hargraeves and Samani, 1982) with a modification for situations where relative humidity is high. Equations (1) and (2) show the formulation used for potential evaporation (PET) computation. In the equation, PET is computed potential evaporation, S is extraterrestrial solar shortwave radiation, R_h is relative humidity, and T_{avg}, T_{min} and T_{max} are measured daily temperature average, minimum, and maximum values..

(1) $$\begin{cases} K_t = \frac{0.0023}{2.5-0.0022\,T_{avg}} & ,R_h < 0.545 \\ K_t = 1.3(1-R_h)^{1/3}\frac{0.0023}{2.5-0.0022\,T_{avg}} & ,R_h \geq 0.545 \end{cases}$$

(2) $$PET = K_t S(T_{avg} + 17.8)(T_{max} - T_{min})^{0.5}$$

Actual evapotranspiration is computed using the computed potential evaporation. The model grid cell contains several water storages, from which the evapotranspiration can happen. The storages are interception storage, soil surface layer storage, and storages in soil layers one and two. The evaporation from interception and soil surface storages is supposed to happen directly, and only after these storages are depleted does the evaporation take place from the soil layers. Evaporation from soil layers is computed using equations (3) and (4), in which $soil_i$ is the water content in soil layer, $smax_i$ is the maximum water content in same soil layer, LAI_{eff} is effective leaf area in the grid cell (equal to half of LAI), E_i is evapotranspiration from the storage, and r_i is fraction of the total amount of roots in the layer in question, and *es* is the evaporation from surface and interception storages.

(3) $$s_i = LAI_{eff}\ soil_i/smax_i$$

(4) $$E_i = (PET - es)r_i(1 - e^{-3.75\,s_i})$$

Leaf area index is computed in the model using a simplified crop growth model based on potential biomass accumulation. The computation method is an adaptation of the commonly used EPIC crop model (Williams *et al.,* 1990). Detailed descriptions of the model equations can be found from the model manual, available from the authors.

S3 Supplementary results

Table S1. Range of changes in monthly discharges for model runs using A1b and B1 emission scenarios from years 2032-2042 compared to baseline 1982-1992.

	Kratie (%)				**Chiang Saen (%)**			
	A1b		B1		A1b		B1	
Month	Range of change		Range of change		Range of change		Range of change	
Jan	-10.3	7.6	-6.9	4.2	-13.5	8.9	-7.2	4.1
Feb	-9.9	4.9	-7.1	2.7	-11.3	5.1	-6.8	-2.5
Mar	-11.3	8.2	-7.7	2.3	-8.7	18.0	-7.1	-0.3
Apr	-9.8	16.1	-5.6	3.3	-3.5	21.3	-5.5	4.2
May	-22.6	32.7	-11.7	18.3	-2.4	8.0	-5.5	7.1
Jun	-28.6	21.9	-15.1	15.7	-4.8	16.5	-9.4	14.3
Jul	-14.7	13.7	-14.0	15.7	-13.5	4.2	-14.9	3.6
Aug	-11.1	6.0	-15.5	8.5	-20.5	5.5	-17.3	-0.9
Sep	-9.4	18.7	-6.4	14.8	-20.7	19.4	-15.7	9.5
Oct	-12.4	25.3	-3.1	20.9	-17.3	27.5	-13.3	1.1
Nov	-10.5	23.3	-4.2	7.8	-15.9	38.4	-13.2	-2.6
Dec	-6.7	19.2	-4.1	4.7	-14.3	16.1	-9.9	-4.2

Table S2: Impact of climate change on Mekong main river discharge (m^3 s^{-1}) in Chiang Saen. Monthly average discharges of the model runs under emission scenarios A1b and B1 (2032-2042) compared to baseline (1982-1992) (see Figure 4A and Figure 4B in main text for graph).

Q [m^3 s^{-1}]	**Baseline**	**A1b**					**B1**				
Month		ccA	cnA	giA	mpA	ncA	ccA	cnA	giA	mpA	ncA
Jan	1,192	1,223	1,030	1,128	1,297	1,284	1,172	1,106	1,116	1,241	1,223
Feb	900	917	799	847	922	947	878	839	846	862	866
Mar	776	789	708	760	915	809	769	721	754	774	746
Apr	752	782	725	771	912	820	783	711	761	745	732
May	979	1,031	956	1,046	1,057	1,040	1,049	1,002	997	938	925
Jun	2,127	2,477	2,025	2,328	2,306	2,356	2,432	2,110	2,269	1,946	1,927
Jul	3,990	4,156	3,452	4,152	3,827	4,081	4,132	3,417	3,928	3,546	3,397
Aug	5,556	5,707	4,420	5,034	5,432	5,861	5,242	4,593	4,907	5,505	4,894
Sep	5,663	5,928	4,494	5,143	5,272	6,761	5,912	4,772	5,076	5,684	6,199
Oct	4,110	4,369	3,400	3,626	5,239	4,221	4,155	3,564	3,776	3,758	3,904
Nov	2,423	2,559	2,039	2,220	3,129	3,354	2,359	2,222	2,249	2,216	2,104
Dec	1,545	1,550	1,324	1,427	1,700	1,793	1,480	1,412	1,442	1,468	1,392

Table S3: Impact of climate change on Mekong main river discharge (m^3 s^{-1}) in Kratie. Monthly average discharges of the model runs under emission scenarios A1b and B1 (2032-2042) compared to baseline (1982-1992) (see Figure 4C and Figure 4D in main text for graph).

Q [m^3 s^{-1}]	**Baseline**	**A1b**					**B1**				
Month		ccA	cnA	giA	mpA	ncA	ccA	cnA	giA	mpA	ncA
Jan	4,273	4,402	3,834	4,116	4,597	4,597	4,224	4,185	3,978	4,444	4,454
Feb	2,956	3,041	2,662	2,854	3,102	3,099	2,945	2,875	2,748	3,037	3,023
Mar	2,147	2,168	1,905	2,052	2,324	2,246	2,126	2,040	1,981	2,193	2,197
Apr	1,652	1,632	1,490	1,610	1,918	1,694	1,663	1,559	1,563	1,706	1,690
May	2,042	2,041	1,580	2,279	2,709	2,453	2,395	2,004	1,802	2,072	2,415
Jun	7,560	9,213	5,397	8,902	7,722	8,938	8,751	7,544	6,523	6,418	7,389
Jul	17,301	19,675	14,759	17,668	16,175	17,693	20,014	16,764	15,596	14,886	15,402
Aug	32,923	34,886	31,468	31,339	29,254	34,386	35,720	34,943	29,738	27,819	31,235
Sep	33,093	39,283	29,993	31,557	36,806	37,685	35,277	32,723	30,967	37,997	36,674
Oct	24,217	29,128	21,219	24,783	30,343	28,321	26,085	23,467	23,962	29,284	28,612
Nov	11,727	13,410	10,493	11,513	14,455	13,475	12,334	11,714	11,231	12,648	12,618
Dec	6,633	7,258	6,192	6,583	7,535	7,909	6,823	6,830	6,362	6,947	6,921

Table S4: Impact of reservoir operation and climate change on Mekong main river discharge (m^3 s^{-1}). Monthly average discharges of the model runs under emission scenarios A1b and B1 (2032-2042) compared to baseline (1982-1992) in Chiang Saen (see Figure 5, Figure 6A, and Figure 6B in main text for graph).

Q [m^3 s^{-1}]	**Baseline**	**Reserv.**	**A1b+rv**					**B1+rv**				
Month	BL	BL+rv	ccA+rv	cnA+rv	giA+rv	mpA+rv	ncA+rv	ccA+rv	cnA+rv	giA+rv	mpA+rv	ncA+rv
Jan	1,192	1,837	1,812	1,664	1,813	1,875	1,863	1,824	1,708	1,763	1,748	1,735
Feb	900	1,675	1,663	1,495	1,651	1,674	1,673	1,685	1,536	1,624	1,526	1,516
Mar	776	1,563	1,578	1,365	1,531	1,599	1,583	1,609	1,452	1,557	1,462	1,447
Apr	752	1,471	1,532	1,199	1,432	1,498	1,531	1,541	1,213	1,443	1,349	1,335
May	979	1,462	1,511	1,079	1,480	1,391	1,531	1,516	1,146	1,398	1,241	1,201
Jun	2,127	1,415	1,540	1,295	1,458	1,503	1,486	1,543	1,308	1,341	1,316	1,287
Jul	3,990	2,103	2,326	1,830	2,107	2,244	2,398	1,975	1,841	2,081	2,117	2,051
Aug	5,556	4,277	4,683	3,572	4,066	4,620	4,861	4,341	3,696	4,017	4,357	3,989
Sep	5,663	4,986	5,277	3,923	4,432	4,868	5,977	5,167	4,125	4,408	4,960	5,181
Oct	4,110	4,016	4,400	3,345	3,574	4,853	4,359	4,149	3,518	3,657	3,693	3,820
Nov	2,423	3,074	3,191	2,899	2,990	3,710	3,977	3,075	3,032	2,981	3,060	2,902
Dec	1,545	2,141	2,123	1,954	2,083	2,283	2,277	2,111	2,045	2,043	2,032	1,968

Table S5: Impact of reservoir operation and climate change on Mekong main river discharge (m^3 s^{-1}). Monthly average discharges of the model runs under emission scenarios A1b and B1 (2032-2042) compared to baseline (1982-1992) in Kratie (see Figure 5, Figure 6C, and Figure 6D in main text for graph).

Q [m^3 s^{-1}]	Baseline	Reserv.	A1b+rv					B1+rv				
Month	BL	BL+rv	ccA+rv	cnA+rv	giA+rv	mpA+rv	ncA+rv	ccA+rv	cnA+rv	giA+rv	mpA+rv	ncA+rv
Jan	4,273	6,038	6,195	5,651	5,985	6,391	6,352	6,069	6,000	5,847	6,161	6,162
Feb	2,956	5,207	5,272	4,917	5,201	5,401	5,316	5,255	5,130	5,051	5,250	5,201
Mar	2,147	4,711	4,709	4,424	4,652	4,920	4,718	4,735	4,606	4,560	4,725	4,660
Apr	1,652	4,342	4,296	4,022	4,343	4,528	4,349	4,398	4,237	4,286	4,363	4,338
May	2,042	4,505	4,508	4,064	4,622	4,831	4,695	4,728	4,453	4,333	4,522	4,646
Jun	7,560	7,472	8,153	5,683	7,849	7,360	8,181	7,904	7,233	6,547	6,516	7,147
Jul	17,301	13,529	15,122	11,098	13,481	12,631	13,823	15,080	13,036	11,834	11,876	12,308
Aug	32,923	25,905	29,336	23,989	25,368	23,810	28,598	29,936	27,623	23,140	21,658	24,700
Sep	33,093	30,663	36,592	27,045	28,797	33,700	35,061	32,934	30,145	27,769	34,019	33,434
Oct	24,217	23,057	27,755	20,001	22,950	27,886	26,550	24,441	21,998	21,867	26,850	26,645
Nov	11,727	13,605	14,977	12,559	13,322	15,905	15,091	13,993	13,368	13,080	14,416	14,331
Dec	6,633	8,448	8,864	7,443	8,282	9,165	9,423	8,531	8,531	7,982	8,727	8,641

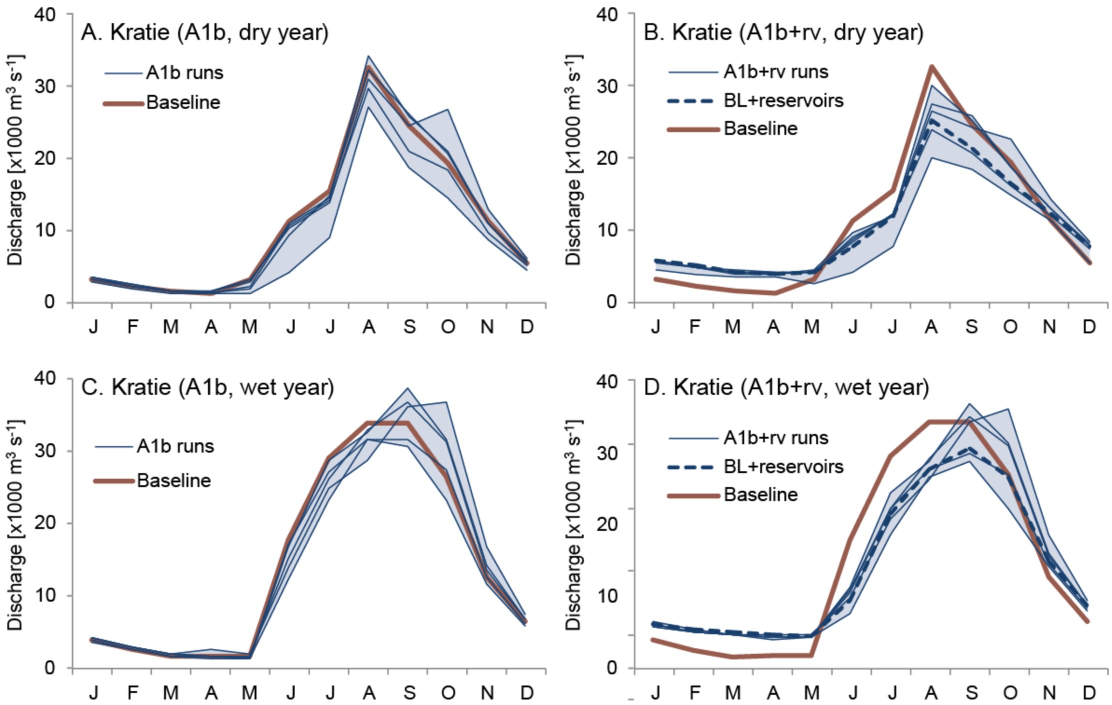

Figure S2: Monthly average discharges at Kratie for: A: dry year (1988) using A1b emission scenario; B: dry year using A1b emission scenario and reservoirs; C: wet year (1990) using A1b emission scenario; and D: wet year using A1b emission scenario and reservoirs.

S4. Comparison of climate change and reservoir operation impact studies

In this section we compare the results of our climate change and reservoir operation assessment to existing assessments carried out in the basin. First we compare the climate change assessments, then we compare reservoir operation (also called in some studies as hydropower development) assessments, and finally we compare the combined climate change and reservoir operation assessments. The comparison has been carried out on flow changes at Chiang Saen and Kratie on monthly or seasonal scales depending on the data availability. The section complements the Discussion Sections 6.1 – 6.3 of the main article.

S4.1 Impacts of climate change

Climate change impacts on the flows of the Mekong have been estimated by Eastham *et al.* (2008), Västilä *et al.* (2010), Hoanh *et al.* (2010), Mekong River Commission (2010b), and Kingston *et al.* (2011). In this section we compare our climate change impact estimates for the flows at Chiang Saen and Kratie with the three first aforementioned studies. The estimates of Kingston *et al.* (2011) and Mekong River Commission (2010b) could not be directly compared due to different scenario formulations and lack of detailed data on their results. Eastham *et al.* (2008) used in their estimations 11 GCMs and the A2 scenario; we compared to these our results from five GCMs and the A1b scenario (Fig. S3). Furthermore, our future climate projection was for the years 2032-2042 and the projection of Eastham *et al.* (2008) was for the year 2030. Västilä *et al.* (2010) and Hoanh *et al.* (2010) used in their estimations the ECHAM4 GCM and scenarios A2 and B2, and therefore we compared our results only from the ECHAM5 GCM and A1b and B1 scenarios. The future climate projection of Västilä *et al.* was for the years 2030-2049, the projection of Hoanh *et al.* (2010) for the years 2010-2050.

The comparison of the assessments at Kratie shows that all four studies in general suggest an increase in flows (Fig. S3, Fig. S4C and S4D), although a few climate models suggest a decrease (Figure S3). The earlier assessments suggest changes in annual flows between -2-82%, whereas our estimate with five GCMs suggests changes between -12-16% in annual flows. In general the estimates of Eastham *et al.* (2008) and Hoanh *et al.* (2010) suggest larger changes than our estimates, but the median of 11 GCMs in the assessment of Eastham et al (2008) shows similarities with the median of five GCMs used in our study (Figure S3). Interestingly the medians of our estimate and the estimate of Eastham *et al.* (2008) suggest that the largest changes in flows will occur during the first (May-June) and last months (September-October) of the monsoon season.

The comparison of the assessments at Chiang Saen shows less agreement in the direction of the flow changes (Fig. S4A and S4B). In the A-scenarios, our assessment agrees with that of Hoanh *et al.* (2010) that the seasonal and annual flows will increase, but in the B-scenarios our assessment suggests a relatively small decrease in flows whilst that of Hoanh *et al.* (2010) suggests an increase. Furthermore, the assessment of Hoanh *et al.* (2010) suggests larger flow changes in both scenarios.

Mekong River Commission (2010b) used only emission scenario B2 and one GCM (ECHAM4). However, as it considered climate change as part of its long-term development scenarios (including hydropower, irrigation and water supply), climate change impacts on hydrology are visible only as part of the development scenarios. At a more general level, however, the report concludes that climate change is likely to bring clearly more variable conditions within the basin as well as increased runoff. The report also states that the expected increase of sea level rise is likely to bring remarkable impacts to the Mekong Delta in Vietnam. Mekong River Commission (2010b) also assessed climate change's impact on the flow from the Mekong River to the Tonle Sap system (the key fisheries production system in the basin, see for example Keskinen, 2006; Mekong River Commission, 2010a). Its estimates indicate that the cumulative impacts of water development and climate change will decrease the average flow volume entering Tonle Sap by around 8%, and that the average date of flow reversal will become almost three weeks earlier when compared to the baseline situation.

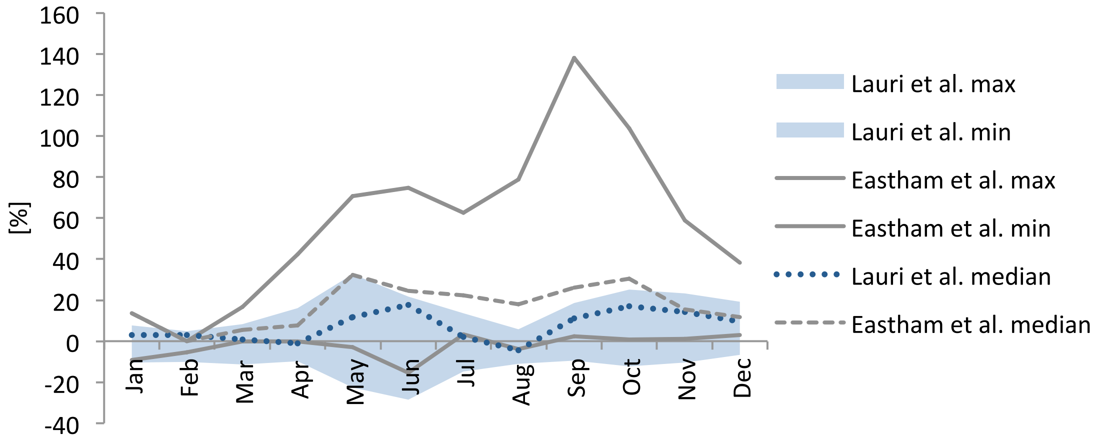

Figure S3. Comparison of climate change impact estimates on flows at Kratie on monthly scale. The compared estimates are ranges and medians of the results from five GCMs of our study and 11 GCMs from Eastham et al. (2008) using the A-scenarios. Lauri et al. refers to this study.

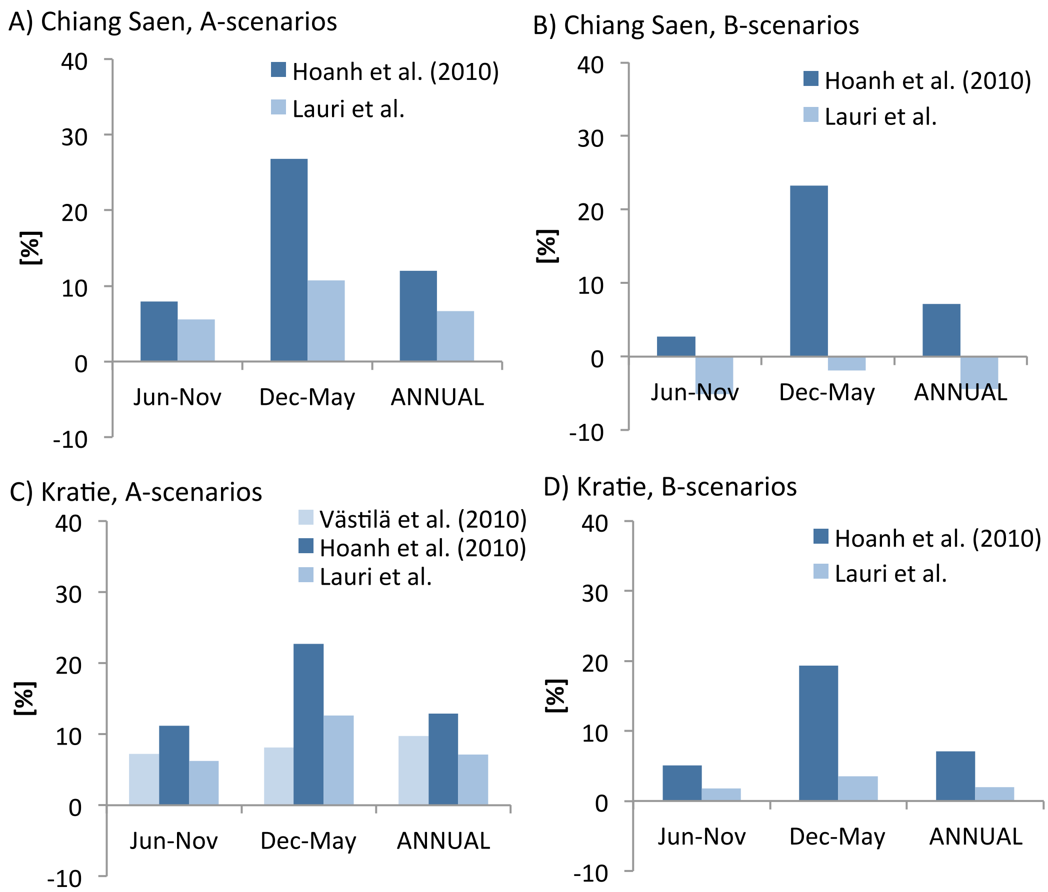

Figure S4. Comparison of climate change impact estimates on flows: A) Chiang Saen, A-scenario; B) Chiang Saen, B-scenario; C) Kratie, A-scenario; and D) Kratie, B-scenarios. Our assessment is based on GCM ECHAM5 and the assessments of Västilä et al. (2010) and Hoanh et al. (2010) are based on GCM ECHAM4. Lauri et al. refers to this study.

S4.2 Impacts of reservoir operation

Reservoir operation impacts on the Mekong's flows have been assessed at Chiang Saen at least by Adamson (2001), Hoanh *et al.* (2010), and Räsänen *et al.* (2012), and at Kratie by ADB (2004) and Hoanh *et al.* (2010). Here, we compare our reservoir operation estimates to these studies. In addition, Mekong River Commission (2010b) included several different scenarios for hydropower (and other) development in the basin. Each study uses different methods to simulate reservoir operations and also the underlying operational assumptions vary: Adamson (2001) used a spreadsheet approach; ADB (2004) used a MikeBasin water resources management tool; Räsänen *et al.* (2012) used a combination of VMod hydrological model and CSUDP dynamic programming tool; Hoanh *et al.* (2011) used a combination of SWAT hydrological model and IQQM water allocation model; and we used a combination of VMod hydrological model and a linear optimisation of reservoir operations. Furthermore, each study used hydrological data from different periods. The baseline data periods were in Adamson (2001) 1960-2001, ADB (2004) 1965-1975, Hoanh *et al.* (2010) 1975-2000, Räsänen *et al.* (2012), and in our study 1982-1992.

At Chiang Saen (Fig. S5A), all assessments agree on the direction of the monthly flow changes relatively well, although there are differences in magnitudes. In general the results of Räsänen *et al.* (2012) suggest the largest changes and our study the smallest changes. On a seasonal scale (Fig. S5B), all assessments suggest similar changes but the assessment of Räsänen *et al.* (2012) suggests the largest changes and the assessment of Hoanh *et al.* (2010) the smallest. Altogether the estimates suggest a 17-22% decrease in June-November flows and 60-90% increase in December-May flows.

At Kratie, our assessment results agree remarkably well, both in magnitude and pattern, with the monthly results of ADB (2004), although some differences exist in May and July (Fig. S6A). On a seasonal scale our results are also well in line with ADB results (Fig. S6B). The results of Hoanh *et al.* (2010) are not fully comparable with the other assessments at Kratie as they also included irrigation in their assessment scenarios. Despite this incompatibility we compared all estimates at Kratie. Altogether the estimates suggest an 8-11% decrease in June-November flows and a 28-71% increase in December-May flows.

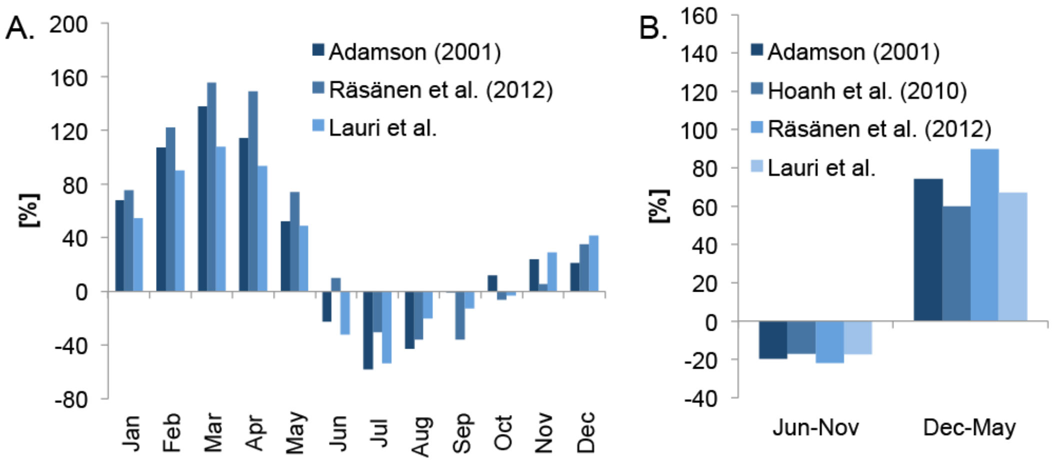

Figure S5. The estimated flow changes at Chiang Saen caused by reservoir operation on A) monthly and B) seasonal scale. Lauri et al. refers to this study.

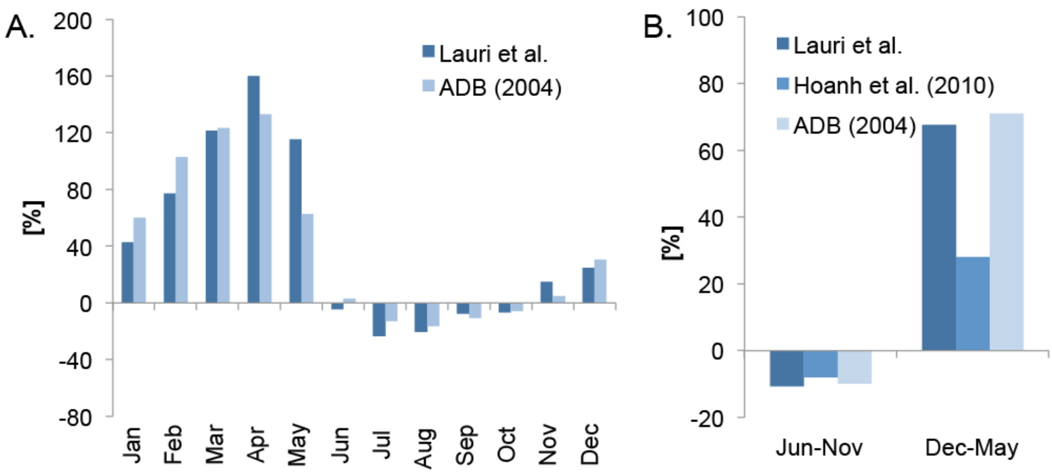

Figure S6. The estimated flow changes at Kratie caused by reservoir operation on A) monthly and B) seasonal scale. Hoanh et al. (2010) also considered irrigation scenarios in their analyses while all other studies only considered impacts of reservoir operation. Lauri et al. refers to this study.

S4.3 Cumulative impacts of climate change and reservoir operation

The combined climate change and reservoir operation impacts on the Mekong's flows have, to the best of our knowledge, so far only been assessed at Chiang Saen and Kratie by Hoanh *et al.* (2010) and Mekong River Commission (2010b). Again, both the estimates of Hoanh *et al.* (2010) and Mekong River Commission (2010b) also incorporate irrigation, and therefore the results at Kratie are not fully comparable with our results. The comparison between Hoanh *et al.* (2010) and our study shows that both studies agree relatively well with the combined impacts on flows at Chiang Saen on a seasonal scale (Fig. S7A and S7B). Both assessments suggest that June-November flows will decrease by 6-18% and that December-May flows will increase by 52-76%. The annual changes vary from a decrease of 4% to an increase of 12%.

The estimates on flow changes at Kratie are somewhat different, but both assessments agree that the December-May flows will increase significantly and annual flows will slightly increase (Fig. S7C and S7D). A more accurate comparison of the results at Kratie would require closer examination on the irrigation scenarios used by Hoanh *et al.* (2010).

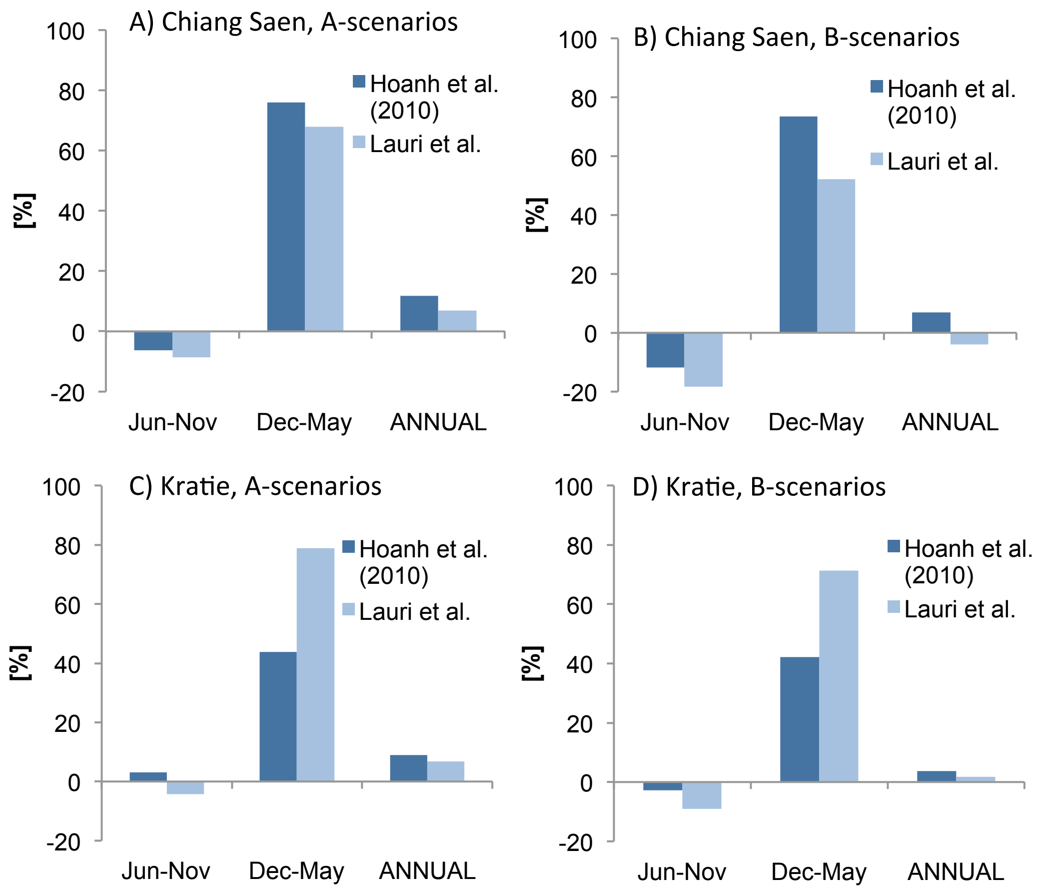

Figure S7. Comparison of combined climate change and reservoir development impact on flow estimates: A) Chiang Saen, A-scenario; B) Chiang Saen, B-scenario; C) Kratie, A-scenario; and D) Kratie, B-scenario. Our assessment is based on GCM ECHAM5 and the assessment of Hoanh et al. (2010) is based on GCM ECHAM4. The estimate of Hoanh et al. (2010) includes the impact of irrigation, which we do not consider in our assessment. Lauri et al. refers to this study.

Mekong River Commission (2010b) estimates that, compared to the baseline situation, the cumulative impact of development scenario for 2060 (including considerable increases in hydropower, irrigation, and water supply) and climate change (scenario B2) will increase remarkably the dry season flows (in March) throughout the basin: up to 105% in Vientiane and 69% in Kratie. The average peak daily flow during the wet season is estimated to decrease in Vientiane by 14%, but increase by 5% in Kratie.

References

ADB: Cumulative impact analysis and Nam Theun 2 contributions, Final report. Prepared by NORPLAN and EcoLao for Asian Development Bank. 143 pp, 2004.

Eastham, J., Mpelasoka, F., Mainuddin, M., Ticehurst, C., Dyce, P., Hodgson, G., Ali, R., and Kirby, M.: Mekong River Basin Water Resources Assessment: Impacts of Climate Change, CSIRO: Water for a Healthy Country National Research Flagship, 2008. http://www.clw.csiro.au/publications/waterforahealthycountry/2008/wfhc-MekongWaterResourcesAssessment.pdf Accessed February 2012

Hargraeves, G. H., and Samani, Z. A.: Estimating potential evapotranspiration, ASCE, J. Irrigation and Drainage Division, 108, 225-230, 1982.

Hoanh, C., Jirayoot, K., Lacombe, G., Srinetr, V.: Impacts of climate change and development on the Mekong flow regime, First assessment – 2009, MRC Technical Paper No. 29 Mekong River Commission, Vientiane, Lao PDR, 2010. http://www.mrcmekong.org/assets/Publications/technical/tech-No29-impact-of-climate-change.pdf Accessed January 2012

Keskinen, M.: The Lake with Floating Villages: A socio-economic analysis of the Tonle Sap Lake, International Journal of Water Resources Development, 22, 463-480, 2006.

Kingston, D. G., Thompson, J. R., and Kite, G.: Uncertainty in climate change projections of discharge for the Mekong River Basin, Hydrology and Earth System Sciences, 15, 1459-1471, 2011.

Mekong River Commission: State of the Basin Report 2010, Mekong River Commission, Vientiane, Lao PDR, 2010a.

Mekong River Commission: Assessment of basin-wide development scenarios –main report, Mekong River Commission (MRC), Vientiane, Lao PDR, 2010b.

Räsänen, T.A., Koponen, J., Lauri, H., and Kummu M.: Downstream hydrological impacts of hydropower development in the Upper Mekong Basin, Water Resources Management, 26, 3495-3513, 2012.

Västilä, K., Kummu, M., Sangmanee, C., and Chinvanno, S.: Modelling climate change impacts on the flood pulse in the Lower Mekong floodplains, Journal of Water and Climate Change, 1, 67-86, 2010.

Williams, J.R., Jones C.A., and Dyke P.T.; The EPIC model documentation. USDA-ARS Technical Bulletin No. 1768. U.S. Department of Agriculture, Washington, DC, 1990